

# The Effect of Tool's Rake Angles and Infeed in Turning Polyamide 66

**Shawbo A. HamaSur**

Department of Mechanical Engineering/Production, College of Engineering, Sulaimani Polytechnic University, Iraq  
shawbo.ali.h@spu.edu.iq

**Rzgar M. Abdalrahman**

Department of Mechanical Engineering/Production, College of Engineering, Sulaimani Polytechnic University, Iraq  
rzgar.abdalrahman@spu.edu.iq (corresponding author)

Received: 28 March 2023 | Revised: 15 May 2023 | Accepted: 17 May 2023

Licensed under a CC-BY 4.0 license | Copyright (c) by the authors | DOI: <https://doi.org/10.48084/etasr.5891>

## ABSTRACT

Polyamide PA66 has been adopted by a variety of industries, and engineering fields. It is used in machinery part production due to its good properties. Machining is the most commonly used processing technique when high quality of part dimension and surface is required. There is a lack of knowledge about the impact of the tool's rake angles when turning polyamide PA66, therefore, this study aims to define an optimal condition that can provide the highest performance in machining polyamide PA66 at the lowest cutting force. The impact of the tool's side rake angle, back rake angle, and cutting depth on cutting force was studied during turning polyamide PA66 with the HSS tool. Three levels were considered for each variable and Taguchi's Orthogonal Array (OA) was used to design nine test configurations. The tests were performed experimentally on a conventional lathe machine. The resultant cutting force was calculated as the response data. The values were converted to signal-to-noise (S/N) ratio to facilitate the analysis using the Taguchi method and analysis of variance (ANOVA). Accordingly, the cutting depth showed the greatest impact on cutting force (57.12%), followed by the side rake angle (27.9%) and back rake angle (8.21%). An optimal condition set to turn polyamide PA66 at the lowest cutting force ( $F_c$ ) is identified as 1 mm depth of cut, side rake angle  $\alpha_s = 21^\circ$ , and back-rake angle  $\alpha_b = 8^\circ$ . Finally, the optimal condition set was evaluated by conformation tests, and the results agreed with the calculations to a large extent.

**Keywords-**polyamide PA66; HSS cutting tool; back rake angle; side rake angle; cutting depth; ANOVA; cutting force

## I. INTRODUCTION

Nowadays, plastics have gained interest in manufacturing various parts of machines due to their good resistance to wear and corrosion, in addition to their low density, coefficient of friction, and high productivity [1, 2]. Polyamide PA66, for instance, is an important thermoplastic type, which is most frequently used in producing power transmission elements (e.g. bearings, cams, worm wheels, gears and bearing cages, slide bearings, gear box parts, and wheel covers parts) in the machinery of different technical sectors including aircraft, automobile, and robotics [3, 4], because, compared to other polymer kinds and despite the aforementioned physical and mechanical properties, it is superior in strength, rigidity, heat stability, chemical resistance, while being a strong noise dampener and electrical insulator [5]. PA66 was introduced as toothbrush filament in 1938 [6]. Polyamides PA66 is one of the most well-known plastics. It consists of two monomers of dicarboxylic and diamine acids [7]. PA66 is a polycondensation product of hexamethylene diammonium and adipate salt. It is

created by removing water from reaction of several species of diamine and diacid [8].

Plastics are less frequently machined. However, the machining process is advised when the quantity of the produced pieces does not warrant the expense of molds [9, 10]. Furthermore, machining the plastic materials is recommended when high quality components with high surface finish and dimensional precision are required [11]. The main aims of the modern machining processes are achieving low power consumption, machining cost, cutting time, cutting force, and stresses with high dimension accuracy, surface quality, tool life, and productivity [12, 13]. The produced cutting forces that act on the cutting tools during the machining are the key component of the machining process responses, their amount has a decisive effect on energy consumption, vibration creation, and the quality of the machined part and cutting tool life [14, 15].

Machining plastic materials needs special processing circumstances to provide acceptable product quality and high

cutting performance. Therefore, this study investigates the effect of tool back rake angle, side rake angle, and cutting depth on the magnitude of cutting force as response data when turning Polyamide PA66. The aim is defining the most proper conditions that ensure lowest cutting force. Three levels are considered for each test parameter and the statistical method of ANOVA is applied for analyzing the obtained response data.

## II. LITERATURE REVIEW

Many machining factors, including cutting conditions and tool geometry, have been considered by researchers to assist in mastering plastic machining, especially polyamide PA66. For instance, authors in [16] investigated the machinability of PA66 polyamide during precision turning at various feed rates. They applied four coated tools of Chemical Vapor Deposition (CVD) coated carbide, Polycrystalline Diamond (PCD), and ISO grade K15 uncoated cemented carbides with and without chip breaker. The findings showed that when turning polyamide PA66 with the K15-KF carbide tool the highest force was recorded, followed by similar results for CVD and PCD, and the lowest force was recorded with the K15 carbide. Authors in [17] performed an experimental and analytical research to examine the surface quality, effective cutting force, and specific cutting pressure under the impact of three test variables of feed, depth of cut, and cutting speed during machining polyamide PA66. The obtained response data were optimized with ANOVA. The statistical results indicated that the feed is the most affecting factor on surface finish followed by cutting speed and cutting depth. The most effective factor on cutting force was the cutting depth ( $d$ ) followed by feed ( $f$ ) and cutting speed ( $V$ ). For a specified cutting force it was  $V$ ,  $f$  and  $d$ , respectively.

Authors in [18] studied experimentally the effect of cutting speed, feed rate, depth of cut, and tool nose radius, when turning polyamide PA-6. Minitab software was used to compile and evaluate the experimental results. Their results show that the feed rate is the most effective factor followed by the cutting depth and tool nose radius, while cutting speed had very little effect on the average surface roughness. Authors in [5] utilized uncoated cemented carbide tools with three different tool nose angles to study the impact of the cutting-edge angles, including angle and nose radius, on the cutting force during turning polyamide PA66. The obtained statistical results concluded that when the included angle is  $35^\circ$  and the simultaneous cutting-edge angles are  $45^\circ$ , the lowest cutting force that offers the most acceptable turning performance was achieved. Additionally, they concluded that the 0.2 mm tool nose radius had the least impact on  $F_c$ . Authors in [19], during turning polyamide PA66, discovered that cutting depth and feed rate have the greatest impact on cutting force. They concluded that as the cutting depth and feed rate rise, the cutting force does as well.

The effects of tool nose radius on tool life, cutting force, temperature, and surface quality were studied in [20] during precise turning of polyamide. The results showed that the cutting force increases with the increase of tool nose radius, while the surface roughness increases with the increase of feed rate and decrease of the tool nose radius. The researchers performed an experimental and analytical investigation to

indicate the influence of feed rate on each of the chip compression ratio, chip deformation, friction angle, shear angle, normal stress, and shear stress of polyamide PA66 during the turning process. They applied uncoated carbide tools without a chip breaker. They concluded that the cutting force presented high values due to the ductile behavior of PA66 polyamide, which is soft and adheres to the tool's rake face. Generally, comparable conclusions were reached when the Merchant model's findings were contrasted with the experimental values [21]. Authors in [22] applied Artificial Neural Networks (ANNs) with Improved Harmony Search Algorithm (IHSA) to determine the optimal cutting parameter set to minimize surface roughness when turning polyamide material. They tested the effect of cutting speed, feed rate, depth of cut, and tool nose radius and found the values of 65.03 m/min, 0.049 mm/rev, 1mm, and 0.8mm, respectively, as the optimal set.

The conclusion of the literature review is that the cutting tool geometry, especially the side and back rake angles, has received less attention in the literature than other aspects of machining of the plastic materials despite its importance in regulating chip formation and flow to reduce cutting forces. Therefore, the current study takes the tool's side and back rake angles with infeed amount into account to define their effectiveness ratio and their optimal set values that provides the lowest cutting force, when turning polyamide PA66.

## III. METHODOLOGY

### A. Materials and Preparation of the Cutting Tools and Specimens

High-Speed Steel (HSS) of 12 mm thickness, grade AISI M2, HS 6-5-2 with 62-65 HRC,  $\zeta\sigma$  selected for preparing different cutting tools with the proposed geometries of the current study, as shown in Figure 1. The tool angles were grounded manually on a tool grinding machine, type Excel, CV7, NW9, ISO 9001, with a swiveling vice, type Vertex, that moves on multiple axes. All the processed tool angles, especially the variables, were checked during and after preparation by the optical projector comparator type Mitutoyo PH-A14 and angle protractors type Mitutoyo with sequential accuracies of 2 minutes and 0.4 minutes to ensure the required tool geometries were obtained exactly.



Fig. 1. The prepared nine HSS cutting tools.

The workpiece material in this study was a polyamide PA66 bar of 750 mm length and 100 mm diameter, supplied by Beijing Feng Teng LTD company, China. The mechanical and physical properties of PA66 are presented in Table I. As shown

in Figure 2, the planned 27 samples were prepared with the dimensions illustrated in Figure 3. Initially, the bar diameter was reduced to 95 mm to ensure producing concentric samples and to reduce the workpiece chattering during testing. The dimensions were checked during and after the sample preparation by precise digital Vernier calipers.

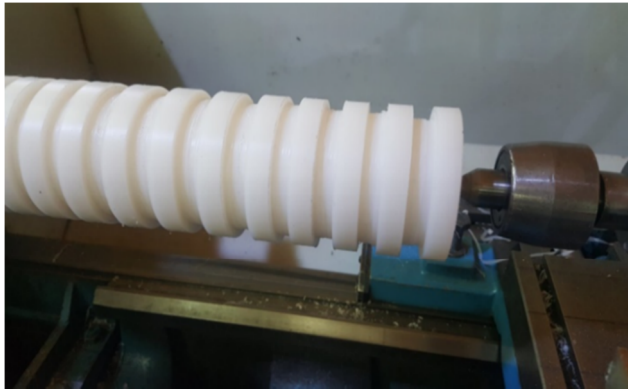


Fig. 2. Prepared samples on the Polyamide PA 66 bar.

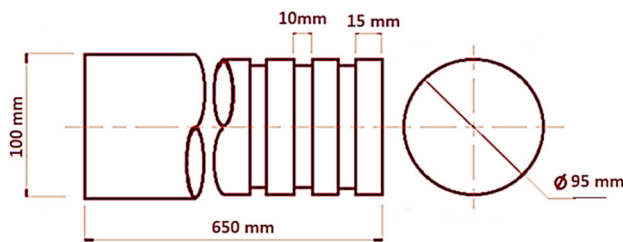


Fig. 3. Dimensions of the prepared samples.

TABLE I. MAIN CHARACTERISTICS OF PA66 [5]

Properties	Units	Tested values
Density	g/cm <sup>3</sup>	1.14
Tensile strength	MPa	60
Coefficient of linear expansion	1/°C	78×10 <sup>-5</sup>
Impact strength	J/m <sup>2</sup>	1400
Rockwell hardness	Kgf / mm <sup>2</sup>	M70-80
Water absorption	-	0.8%

**B. Test Devices**

The tests were performed on a universal lathe machine type CU630-3000, serial number 1270 with a 15 hp driving motor. A dial gauge was mounted at the back of the cross slide to further ensure the compound rest accuracy. The cutting forces were measuring by a 3D (x, y, z) dynamometer of 500 kg (5000N) capacity and 1 Kgf (10 N) resolution. The device was provided by Unitech Scales and Measurements Pvt. Ltd. India. It consists of strain gauges as sensing elements connected by a Whetstone’s based 350 Ω bridge. The software Tool Viewer V2.1 was installed on a computer to log the received data from a data acquisition system connected to the dynamometer. In order to guarantee the correctness of the tests results, the lathe machine and all the used equipment in this test rig (Figure 4) were subjected to calibration and maintenance.

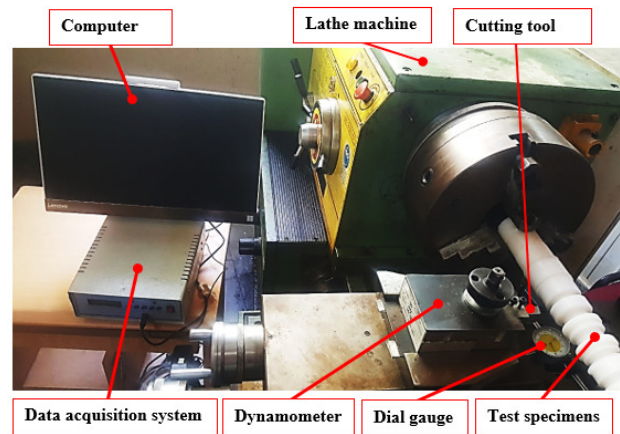


Fig. 4. Test devices.

**C. Design of the Experiments**

In the current study, the back ( $\alpha_b$ ) and side ( $\alpha_s$ ) rake angles of the cutting tool along with the cutting depth (Figure 5) [23], were selected as variables during turning Polyamide PA66. The other tool geometries, i.e. nose radius, side and end cutting edge angles, cutting speed, and feed rate, were kept constant at 1 mm, 3°, 12°, 300 rpm, and 0.25 mm/rev, respectively. Three levels were proposed for each variable (Table II). Consequently, in order to perform the lowest test number for investigating the quality properties, the standard Taguchi’s L9 (3×3) Orthogonal Array (OA) was applied to design 9 experiment combinations, as shown in Table III. The values of all the variables and constant parameters were suggested according to the literature and specific test results. The test of each designed experiment was repeated at least three times to ensure the accuracy of the results.

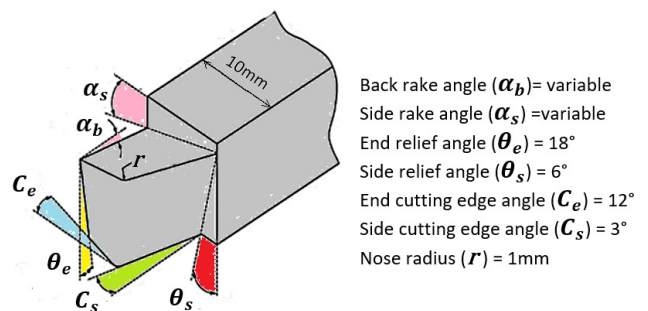


Fig. 5. Single point cutting tool geometry.

TABLE II. PROPOSED PARAMETERS AND THEIR LEVELS

Factors	Unit	Levels			
		1	2	3	
Side rake angle ( $\alpha_s$ )	A	°	7	14	21
Back rake angle ( $\alpha_b$ )	B	°	0	4	8
Cutting depth	C	mm	1	2	3

**D. Analysis of Variance**

Cutting force ( $F_c$ ) is an essential evaluator for the machining performance, therefore it is regarded as the response

variable in the current study. After performing the planned tests, the Mean Square Deviation (MSD) of the  $F_c$  results in each trail (Table III), were determined as [19]:

$$MSD = \frac{1}{r} \sum_{i=1}^n y_i^2 \quad (1)$$

The smaller the  $F_c$  value, the lower the power consumption and the vibration and the higher the tool life and product quality [20]. Accordingly, in order to facilitate the evaluation of the LB features of the proposed characters, the basis of "smaller is better" (LB) was considered to convert the MSD values to signal to noise ratio (S/N) by [24]:

$$S/N = 10 \times \text{LOG}_{10} (MSD) \quad (2)$$

TABLE III. DESIGNED EXPERIMENTS ACCORDING TO TAGUCHI'S L9 OA

Trail No.	Parameters and levels			Response variable	
	A	B	C	MSD	S/N ratio
				N	dB
1	1	1	1	95.1	-39.6
2	1	2	2	140	-42.9
3	1	3	3	154.5	-43.8
4	2	1	2	129.5	-42.2
5	2	2	3	132.5	-42.4
6	2	3	1	80	-38.1
7	3	1	3	130	-42.3
8	3	2	1	73.6	-37.3
9	3	3	2	73	-37.3

The average performance of each specified level of the variables is defined by the mean of the S/N ratios of the trails that contain the entire level, as presented in Table IV. Also, the difference between the highest and lowest average performance of each variable was determined to define its rank and importance. Based on the results showed in Table IV, the ANOVA statistical method was applied to define the individual significance of the proposed variables in influencing the response data of cutting force as shown in Table V.

TABLE IV. AVERAGE PERFORMANCE OF THE VARIABLE LEVELS

Level	$\alpha_s$ (°)	$\alpha_b$ (°)	Cutting depth (mm)
	A	B	C
1	-42.1	-41.4	-38.3
2	-40.9	-40.9	-40.8
3	-39.0	-39.7	-42.8
$L_{max} - L_{min}$	2.0	1.7	4.5
Ranking	2	3	1

TABLE V. ANOVA RESULTS

Source	Degrees of Freedom	Sum of Squares	Variance	Variance ratio	Percentage contribution
	DoF	SS	V	F-test	P %
A	2	15.0	7.5	4.1	27.9
B	2	4.4	2.2	1.2	8.2
C	2	30.7	15.3	8.5	57.1
Residual error	2	3.6	1.8	1.0	6.8
Total	8	53.7			

IV. RESULTS

Figure 6 presents the attributes of the machining force components for a test in the first trail when turning a Polyamide 66 sample. It shows that the tangential force ( $F_t$ ) is the largest, and each of the feed ( $F_f$ ) and infeed ( $F_r$ ) component values are almost a quarter of the  $F_t$  value. All the force components initiate at point (a), where the cutting edge, as illustrated in Figure 7(A), is initially contacting the sample. The forces are noticeably rising simultaneously with increasing the workpiece/cutting edge contact length to its maximum value at point (b) and remains constant till point (c). Therefore, the effective values of  $F_t$ ,  $F_f$ , and  $F_r$  in each test, were calculated as their averages in this period. After point (c), the forces start dropping inconsistently due to the gradual reduction of the contact length. The inconsistent drop is the result of spinning instead of cutting the remained weak triangular section layer of the material, as illustrated in Figure 7(B). The effective cutting force ( $F_c$ ) in the current study is calculated as the resultant of the effective components of  $F_t$ ,  $F_f$ , and  $F_r$  by [25]:

$$F_c = \sqrt{F_t^2 + F_f^2 + F_r^2} \quad (3)$$

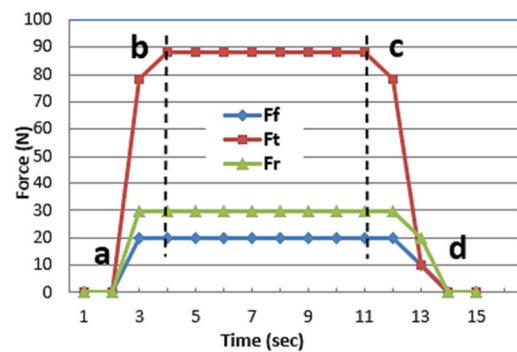


Fig. 6. Cutting force results of a test in the first trail ( $\alpha_s = 7^\circ$ ,  $\alpha_b = 0^\circ$ ,  $d = 1\text{mm}$ ).

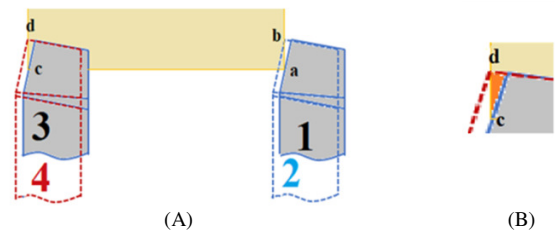


Fig. 7. The cutting pass during the tests.

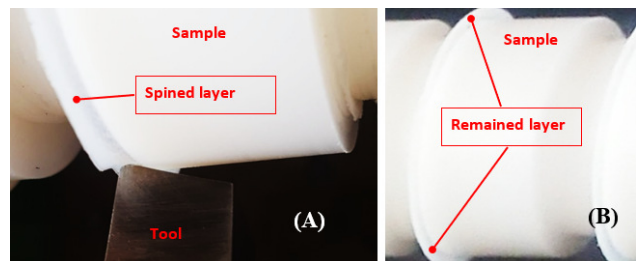


Fig. 8. The remained layer of the work material at the sample end (A) before and (B) after spinning.



The average performance of the S/N of each variable's level is presented in Figure 9. Accordingly, the optimal combination of  $\alpha_s$ ,  $\alpha_b$ , and the infeed can be defined as the third level of  $\alpha_s$  ( $A_3 = 21^\circ$ ), third level of  $\alpha_b$  ( $B_3 = 8^\circ$ ), and first level of cutting depth ( $C_1=1\text{mm}$ ), represented as A3B3C1. The significance of the proposed factors of cutting depth, side rake angle, and back rake angle in addition to their role in turning PA66 with the lowest cutting force value are determined by the ANOVA. Table V defines the ANOVA results of all the variables. The contribution percentage results, shown in Figure 10, illustrate that the cutting depth contributes by 57.12% in affecting the cutting force and it is the most important factor, followed by the side rake angle, which has an effectiveness of 27.9%, and the back rake angle which has the least impact of 8.21%.

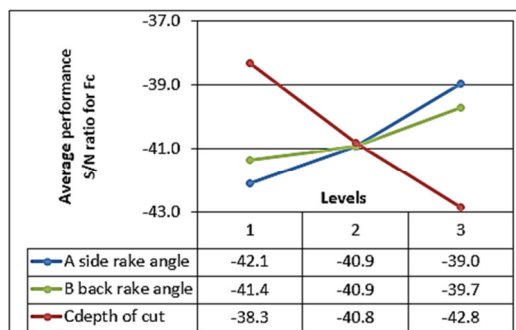


Fig. 9. Average performance of the variable levels.

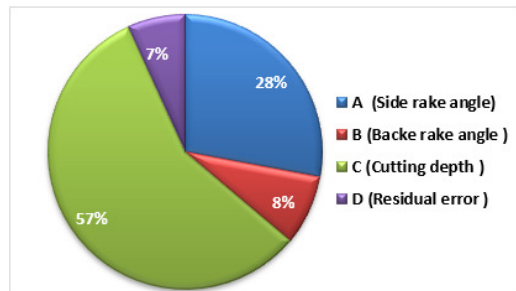


Fig. 10. Contribution percentage of the factors in affecting the  $F_c$ , besides the residual error.

While the deduced optimal combination set of A3B3C1 did not exist in the 9 designed tests in this study, its value in S/N ratio was predicted as [19]:

$$Y_{opt} = T/N + (A_3 - T/N) + (B_3 - T/N) + (C_1 - T/N) \quad (4)$$

Accordingly, the calculated response value of the optimal set is -35.67 dB (60.76 N), which is smaller than the lowest value in Table III. This confirms the validity of the concluded optimal condition set. Then, the confidence value of 90% was depended to determine the confidence interval (C.I.) of  $\pm 0.97$  dB by [19]:

$$C.I. = \pm \sqrt{F(1, n_2) \times (V_e/N_e)} \quad (5)$$

The C.I. value shows that the experimental performance of the defined optimal set will be between -34.30 dB (51.88 N) and -36.26 dB (65.16 N). Finally, the  $F_c$  value of the confirmation test of 59 N (-35.41 dB) was obtained. It confirms

the correctness of the concluded optimal combination set, because the deduced experimental  $F_c$  value is within the confidence limits of the expected value.

### V. DISCUSSION

The experimental results of this research showed that the most effective factor on cutting force is the cutting depth, in accordance with the findings in [17, 19, 20]. Authors in [5] obtained lowest cutting force at lowest simultaneous cutting-edge angles of  $45^\circ$  without noticing inconsistent drop in the forces at the end of the cutting passes, as was occurred in the current study. That can be interpreted due to the fact that the large approach angle reduces the amount of remained material layer at the end of the passes.

The optimal set obtained in this study not only facilitates the cutting of PA66 with minimal force, but also enables machining PA66 with lowest power consumption, machining cost, cutting time, cutting stresses and highest part quality, tool life, and productivity. The produced cutting forces are an essential evaluator for the aforementioned machining performances as deduced in [22].

### VI. CONCLUSION

This study aimed to find an optimum combination set of cutting depth, side rake angle, and back rake angle for turning polyamide PA66 at the lowest cutting force ( $F_c$ ) value. Three levels for each variable were considered. Taguchi's L9 OA was applied to set the experiments. The obtained  $F_c$  results were transferred to signal to noise ratio (S/N) to facilitate analyzing by ANOVA and the following were concluded:

- The cutting depth has the maximum contribution factor of 57.12% in generating the resultant cutting force. The side rake angle has an effect of 27.9%, while the back rake angle has the lowest contribution of 8.21%.
- The optimum condition set of factor combination that provides minimal cutting force is the cutting depth of 1 mm, side rake angle of  $21^\circ$ , and back rake angle of  $8^\circ$ .
- The experimental confirmation test result of the  $F_c$  value confirmed the correctness of the concluded optimal condition and its expected result.

### ACKNOWLEDGMENT

The authors are greatly thankful to the staff of the Workshops and the Metal Cutting Lab of the Mechanical Engineering Department, Polytechnic University, Sulaimani, for their help and support. Special thanks go to Mr. Barzan Talib for his advice and guidance.

### NOMENCLATURE

C.I.	Confidence Interval	n	Number of observations of the results
F	Variance ratio	$n_2$	Error DoF $n_2 = f_e$
$F_f$	Feed force	r	From Taguchi's table and its always 1
$F_r$	Radial force	S/N	Signal to noise ratio
$F_t$	Tangential force	T	Sum of the S/N ratio
$f_e$	Degree of freedom of the error term	$V_e$	Variance of the error term

MSD	Mean Square Deviation	$\gamma_i$	Resulting value of the cutting force
$N$	Total number of trials or number of S/N ratio	$\alpha_b$	Back rake angle
$N_e$	Effective number of replications	$\alpha_s$	Side rack angle

## REFERENCES

- [1] N. Dusunceli and O. U. Colak, "The effects of manufacturing techniques on viscoelastic and viscoplastic behavior of high density polyethylene (HDPE)," *Materials & Design*, vol. 29, no. 6, pp. 1117–1124, Jan. 2008, <https://doi.org/10.1016/j.matdes.2007.06.003>.
- [2] D. G. Zisopol, A. I. Portoaca, I. Nae, and I. Ramadan, "A Comparative Analysis of the Mechanical Properties of Annealed PLA," *Engineering, Technology & Applied Science Research*, vol. 12, no. 4, pp. 8978–8981, Aug. 2022, <https://doi.org/10.48084/etasr.5123>.
- [3] J. C. Won, R. Fulchiron, A. Douillard, B. Chabert, J. Varlet, and D. Chomier, "Effect of the pressure on the crystallization behavior of polyamide 66," *Journal of Applied Polymer Science*, vol. 80, no. 7, pp. 1021–1029, 2001, <https://doi.org/10.1002/app.1185>.
- [4] B. L. Deopura, R. Alagirusamy, M. Joshi, and B. Gupta, *Polyesters and Polyamides*. Boca Raton, FL, USA: CRC Press, 2008.
- [5] P. Sidiq, R. M. Abdalrahman, and S. Rostam, "Optimizing the simultaneous cutting-edge angles, included angle and nose radius for low cutting force in turning polyamide PA66," *Results in Materials*, vol. 7, Sep. 2020, Art. no. 100100, <https://doi.org/10.1016/j.rinma.2020.100100>.
- [6] J. Koech, E. Omollo, F. Nzioka, and J. Mwasiagi, "Thermal Analysis of Polyamide-66/POSS nanocomposite fiber," *International Journal of Engineering and Technical Research*, vol. 7, no. 4, Apr. 2017, Art. no. 265036.
- [7] Z. Zakaria, Z. Izzah, M. Jawaid, and A. Hassan, "Effect of degree of deacetylation of chitosan on thermal stability and compatibility of chitosan-polyamide blend," *BioResources*, vol. 7, no. 4, pp. 5568–5580, 2012.
- [8] R. A. Ortega, E. S. Carter, and A. E. Ortega, "Nylon 6,6 Nonwoven Fabric Separates Oil Contaminates from Oil-in-Water Emulsions," *PLOS ONE*, vol. 11, no. 7, Jun. 2016, Art. no. e0158493, <https://doi.org/10.1371/journal.pone.0158493>.
- [9] D. G. Zisopol, I. Nae, A. I. Portoaca, and I. Ramadan, "A Statistical Approach of the Flexural Strength of PLA and ABS 3D Printed Parts," *Engineering, Technology & Applied Science Research*, vol. 12, no. 2, pp. 8248–8252, Apr. 2022, <https://doi.org/10.48084/etasr.4739>.
- [10] D. G. Zisopol, M. Minescu, and D. V. Iacob, "A Theoretical-Experimental Study on the Influence of FDM Parameters on the Dimensions of Cylindrical Spur Gears Made of PLA," *Engineering, Technology & Applied Science Research*, vol. 13, no. 2, pp. 10471–10477, Apr. 2023, <https://doi.org/10.48084/etasr.5733>.
- [11] P. K. Roy and S. K. Basu, "Evaluation of processing factors on turning of thermoplastics," *Polymer Engineering & Science*, vol. 17, no. 10, pp. 751–757, 1977, <https://doi.org/10.1002/pen.760171010>.
- [12] V. N. Gaitonde, S. R. Karnik, F. Mata, and J. P. Davim, "Taguchi Approach for Achieving Better Machinability in Unreinforced and Reinforced Polyamides," *Journal of Reinforced Plastics and Composites*, vol. 27, no. 9, pp. 909–924, Jun. 2008, <https://doi.org/10.1177/0731684407085875>.
- [13] N. V. Cuong and N. L. Khanh, "Improving the Accuracy of Surface Roughness Modeling when Milling 3x13 Steel," *Engineering, Technology & Applied Science Research*, vol. 12, no. 4, pp. 8878–8883, Aug. 2022, <https://doi.org/10.48084/etasr.5042>.
- [14] N. A. Fountas, I. Ntziantzias, J. Kechagias, A. Koutsomichalis, J. P. Davim, and N. M. Vaxevanidis, "Prediction of Cutting Forces during Turning PA66 GF-30 Glass Fiber Reinforced Polyamide by Soft Computing Techniques," *Materials Science Forum*, vol. 766, pp. 37–58, 2013, <https://doi.org/10.4028/www.scientific.net/MSF.766.37>.
- [15] H. K. Le, "Multi-Criteria Decision Making in the Milling Process Using the PARIS Method," *Engineering, Technology & Applied Science Research*, vol. 12, no. 5, pp. 9208–9216, Oct. 2022, <https://doi.org/10.48084/etasr.5187>.
- [16] J. Paulo Davim, L. R. Silva, A. Festas, and A. M. Abrão, "Machinability study on precision turning of PA66 polyamide with and without glass fiber reinforcing," *Materials & Design*, vol. 30, no. 2, pp. 228–234, Feb. 2009, <https://doi.org/10.1016/j.matdes.2008.05.003>.
- [17] S. Haoues, M. A. Yallese, S. Belhadi, S. Chihaoui, and A. Uysal, "Modeling and optimization in turning of PA66-GF30% and PA66 using multi-criteria decision-making (PSI, MABAC, and MAIRCA) methods: a comparative study," *The International Journal of Advanced Manufacturing Technology*, vol. 124, no. 7, pp. 2401–2421, Feb. 2023, <https://doi.org/10.1007/s00170-022-10583-8>.
- [18] D. Lazarevic, P. Jankovic, M. Madic, and A. Lazaravic, "Study on surface roughness minimization in turning of polyamide PA-6 using Taguchi method," in *34th International Conference on Production Engineering*, Nis, Serbia, Sep. 2011, pp. 515–518.
- [19] M. Marin, "Studies on the main cutting force in turning polyamide PA66," in *Annals of the Oradea University: Fascicle Management and Technological Engineering*, Oradea, Romania: University of Oradea, 2010, pp. 3.162-3.166.
- [20] L. R. Silva and J. P. Davim, "The Effect of Tool Geometry on the Machinability of Polyamide During Precision Turning," *Journal of Composite Materials*, vol. 43, no. 23, pp. 2793–2803, Nov. 2009, <https://doi.org/10.1177/0021998309345310>.
- [21] L. R. Silva, J. P. Davim, A. M. Abrão, and P. E. Faria, "Merchant Model Applied to Precision Orthogonal Cutting of Pa66 Polyamide with and without Glass Fiber Reinforcing," *Journal of Composite Materials*, vol. 43, no. 23, pp. 2727–2737, Nov. 2009, <https://doi.org/10.1177/0021998309345312>.
- [22] M. Madic, D. Markovic, and M. Radovanovic, "Optimization of Surface Roughness When Turning Polyamide using ANN-IHSA Approach," *International Journal of Engineering & Technology*, vol. 1, no. 4, pp. 432–443, Sep. 2012, <https://doi.org/10.14419/ijet.v1i4.378>.
- [23] I. P. Girsang and J. S. Dhupia, "Machine Tools for Machining," in *Handbook of Manufacturing Engineering and Technology*, A. Y. C. Nee, Ed. London, UK: Springer, 2015, pp. 811–865.
- [24] R. K. Roy, *A Primer on the Taguchi Method*, 2nd Edition. Southfield, MI, United States: Society of Manufacturing Engineers, 2010.
- [25] M. Rizal, J. A. Ghani, and A. Z. Mubarak, "Design and Development of a Tri-Axial Turning Dynamometer Utilizing Cross-Beam Type Force Transducer for Fine-Turning Cutting Force Measurement," *Sensors*, vol. 22, no. 22, Jan. 2022, Art. no. 8751, <https://doi.org/10.3390/s22228751>.